



**HAL**  
open science

## Absolute calibration of radar altimeters : consistency with electromagnetic modelling

G rard Caudal, Emmanuel P. Dinnat, Jacqueline Boutin

► **To cite this version:**

G rard Caudal, Emmanuel P. Dinnat, Jacqueline Boutin. Absolute calibration of radar altimeters : consistency with electromagnetic modelling. *Journal of Atmospheric and Oceanic Technology*, 2005, 22 (6), pp.771-781. 10.1175/JTECH1743.1 . hal-00145776

**HAL Id: hal-00145776**

**<https://hal.science/hal-00145776>**

Submitted on 1 Mar 2021

**HAL** is a multi-disciplinary open access archive for the deposit and dissemination of scientific research documents, whether they are published or not. The documents may come from teaching and research institutions in France or abroad, or from public or private research centers.

L'archive ouverte pluridisciplinaire **HAL**, est destin e au d p t et   la diffusion de documents scientifiques de niveau recherche, publi s ou non,  manant des  tablissements d'enseignement et de recherche fran ais ou  trangers, des laboratoires publics ou priv s.

## Absolute Calibration of Radar Altimeters: Consistency with Electromagnetic Modeling

GÉRARD CAUDAL

*CETP/IPSL, Vélizy, France*

EMMANUEL DINNAT

*ESTEC/European Space Agency, Noordwijk, Netherlands*

JACQUELINE BOUTIN

*LODYC/IPSL, Paris, France*

(Manuscript received 12 December 2003, in final form 21 July 2004)

### ABSTRACT

Empirical Ku-band altimeter model functions of near-nadir normalized radar cross-sectional  $\sigma^{\circ}$  are compared to electromagnetic two-scale quasi-specular theory in the context of a standard sea wave spectral model. Three empirical model functions are tested: (i) the modified Chelton and Wentz model (WCM) using data from *Geosat*, (ii) the Callahan et al. model using data from TOPEX, and (iii) the Freilich and Vanhoff model using data from the Tropical Rainfall Measuring Mission (TRMM) precipitation radar (PR). These three models are basically very similar, except that they differ in terms of the level of absolute calibration. The difference between the absolute calibrations of the two extreme models (MCW and Freilich and Vanhoff) is as high as 1.9 dB. Assuming a sea wave spectrum similar to that used by Elfouhaily et al., the two-scale quasi-specular electromagnetic model is run, with a wave separation wavenumber  $k_d$  adjusted so as to minimize the rms difference between the theoretical  $\sigma^{\circ}(\theta)$  function and the empirical near-nadir model function. The quality of the best-fit solution is not perfect, however, because the shape and absolute level of the function  $\sigma^{\circ}(\theta)$  cannot usually be adjusted simultaneously by the electromagnetic model. Taking the model function used by Freilich and Vanhoff as a reference, an offset is then introduced to the empirical model function, and the residual error is computed as a function of the offset. The overall quality of the fit is shown to be best when a  $-1.1$  dB offset is introduced into the Freilich and Vanhoff model function. To within 0.1 dB, this corresponds to the offset that would be required to match Callahan et al.'s model function. This result is obtained in a context where the effect of the peakedness of the sea surface was assumed negligible. When this effect is introduced, with a peakedness parameter  $\Delta$  assumed to be independent of wind speed and taken tentatively as  $\Delta = 0.23$ , as suggested by Chapron et al., the optimal offset is then found to be  $-0.2$  dB, thus indicating that for this example the best consistency with electromagnetic modeling is closer to Freilich and Vanhoff's calibration. A more refined assessment would require accurate measurements of the parameter  $\Delta$  involving both magnitude and variability with wind speed. Such accurate measurements are, unfortunately, not available at this time.

### 1. Introduction

Measurements of the normalized radar cross-sectional  $\sigma^{\circ}$  are currently being performed from satellite or aircraft in order to retrieve the small-scale properties of the sea surface. While scatterometers measure  $\sigma^{\circ}$  at incidence angles principally above  $20^{\circ}$ , altimeters oper-

ate with incidence angles close to  $0^{\circ}$ . From the observations performed in both modes, empirical models have been produced in order to relate the normalized radar cross-sectional  $\sigma^{\circ}$  to the wind speed above the ocean at various microwave frequencies. This paper focuses on Ku-band altimetry, which has been the topic of many investigations (see the review by Chelton et al. 2001). When dealing with wind speed algorithms, an important issue of radar altimetry is the question of absolute calibration and much work has been devoted to this problem. In that context, a study involving cross

---

Corresponding author address: Gérard Caudal, CETP/IPSL, 10-12 Ave. de l'Europe, 78140 Vélizy, France.  
E-mail: gerard.caudal@cetp.ipsl.fr

calibration between *Geosat* and *Seasat* altimeter estimates was performed by Witter and Chelton (1991). They concluded that the *Seasat* altimeter estimates were miscalibrated and proposed a modification to the altimeter model function previously proposed by Chelton and Wentz (1986). Comparing TOPEX/Poseidon and *Geosat* altimeter measurements, Callahan et al. (1994) identified an offset of 0.7 dB between both datasets. They were able to interpret this offset as a consequence of corrections (round earth correction, atmospheric absorption) that had not been taken into account in the *Geosat* data. More recently, Freilich and Vanhoff (2003) used measurements from the Tropical Rainfall Mapping Mission (TRMM) precipitation radar (PR) to construct a fully empirical model function relating a near-nadir radar cross section to wind speed. They found that their TRMM PR model function compared well with TOPEX and *Geosat* results (Witter and Chelton 1991; Freilich and Challenor 1994), except that it exhibited a  $\cong +1.9$  dB offset.

Recently, an important effort has been done by European Space Agency (ESA) to produce an absolute calibration for the European Space Agency's *Environmental Satellite (ENVISAT)* Ku-band radar altimeter, based on the use of a transponder (Robinson 2000), or using a passive calibration method formerly developed for the *European Remote Sensing Satellite-1 (ERS-1)* altimeter (Greco et al. 2000). For example, a difference of 0.91 dB is found between preflight calibration and in-flight calibration of the *ENVISAT* Ku-band radar altimeter receiver gain based on the passive calibration method (B. Greco 2004, personal communication). Although no model function is yet available from the *ENVISAT* radar altimeter for inclusion in this paper, such a difference illustrates the difficulty in obtaining accurate absolute calibration of radar altimeters, thus leading to the offset found between different model functions elaborated from various satellites.

Since it is not possible to attribute the +1.9 dB offset between the TRMM PR model and previous model functions to calibration error of one specific satellite, this discrepancy points out some of the uncertainty with which the model function is presently used. Since this offset is quite substantial, it seems to be useful to explore whether such an offset either improves or debases the consistency of the model function with the  $\sigma^\circ$  expected theoretically from electromagnetic modeling. As a matter of fact, the radar altimeter empirical model functions involve the shape of the profile of  $\sigma^\circ$  as a function of incidence angle  $\theta$  close to nadir ( $\theta = 0^\circ$  to  $18^\circ$ , typically), as well as its absolute level. It turns out that requiring both types of observations (profile and absolute level of  $\sigma^\circ$ ) to be matched simultaneously by

means of electromagnetic modeling is not always possible. Assuming that the shape of the  $\sigma^\circ(\theta)$  profile is correctly reproduced by empirical models, then the required consistency with electromagnetic modeling puts strong constraints on the absolute level of  $\sigma^\circ$ . This paper presents these constraints and gives some indications of the order of magnitude of an offset that would be consistent with standard electromagnetic modeling.

Recently, Anderson et al. (2000) performed a very comprehensive study involving the comparison between empirical model functions and physically based backscatter models [see also a briefer report by Anderson et al. (2002)]. This allowed them to study notably the impact of sea state on radar backscatter in order to improve the wind field retrieval from radar remote sensing. As far as radar altimetry is considered, Anderson et al.'s comparisons between empirical and physically based models were limited to a comparison of  $\sigma^\circ$  at nadir ( $\theta = 0^\circ$ ). In the present work, the effect of sea state on  $\sigma^\circ$  is not discussed (the fully developed situation is assumed to be representative of the open ocean probed by satellite radar altimeters). However, unlike Anderson et al., the constraints introduced here by considering not only  $\sigma^\circ(\theta = 0)$  but also the shape of the profile  $\sigma^\circ(\theta)$  in the vicinity of  $\theta = 0$  allow us to discuss the consistency of the absolute calibrations of radar altimeters.

## 2. Electromagnetic modeling

### a. Two-scale quasi-specular model

Theoretical models of the interaction between electromagnetic waves and random surfaces have been developed in order to help interpret the observations. For near-nadir observations, the quasi-specular approach (Barrick 1968) relates  $\sigma^\circ$  to the slope probability density function (pdf) via the Fresnel reflection coefficient. It was further recognized that a two-scale approach was necessary, as reviewed by Valenzuela (1978). The two-scale approach requires the introduction of a cutoff wavenumber  $k_d$ . Then, the near-nadir  $\sigma^\circ$  is expressed according to

$$\sigma^0(\theta) = |R'(0)|^2 \pi \frac{p(\tan\theta, 0)}{\cos^4\theta}, \quad (1)$$

where  $\theta$  is the incidence angle and  $R'(0)$  is the Fresnel reflection coefficient for normal incidence, corrected in order to account for diffraction effects due to the small-scale roughness. The function  $p(\xi_x, \xi_y)$  is the sea surface slope pdf of ocean waves whose wavenumbers are smaller than  $k_d$ , and direction  $x$  is oriented toward the

radar-viewing direction, while direction  $y$  is perpendicular to  $x$ .

Assuming for instance an isotropic rough surface of Gaussian slope pdf with an effective mean square slope  $s^2$  (obtained by integrating the slope spectrum over the domain of wavenumbers smaller than  $k_d$ ), expression (1) can be rewritten as

$$\sigma^o(\theta) = \frac{|R'(0)|^2}{s^2 \cos^4 \theta} \exp(-\tan^2 \theta/s^2). \quad (2)$$

Although the two-scale quasi-specular model provides a very simple formulation of the near-nadir backscatter, it is unable by itself to yield the appropriate values of  $k_d$  and  $R'(0)$ . It turns out, however, that for near-nadir incidences the modeled  $\sigma^o$  is substantially affected by the choice of  $k_d$ . Jackson et al. (1992) proposed a ratio of the electromagnetic wavenumber  $k_o$  to  $k_d$  of the order of 3–6, on the basis of a comparison with the physical optics approach in the infinite conductivity case.

*b. Diffraction-modified Fresnel coefficient*

In the framework of polarimetric passive remote sensing of the sea surface, Yueh et al. (1994) and Yueh (1997) have developed the small perturbation method (SPM) to second order for randomly rough surfaces. The scattered field is decomposed into coherent and incoherent components. The zero-order scattered field is a coherent field propagating in the specular direction, and its amplitude is characterized by the Fresnel reflection coefficients  $R_{HH}^{(0)}$  and  $R_{VV}^{(0)}$  for horizontal and vertical polarizations, respectively. While the first-order scattered field is incoherent, the second-order scattered field is coherent and gives a correction to the Fresnel coefficient. For HH and VV polarizations the coherently scattered field should be largely dominant in the vicinity of the specular direction, and since we are dealing with near-nadir observations, the incoherent component will be ignored in our analysis. To assess the range of validity of this approximation, one may refer to the work by Jackson et al. (1992), who compared the two-scale model approximation with the solution of the physical optics (PO) integral performed in the perfect conductivity case. They obtained that the two-scale quasi-specular model approximates the PO integral to within a few percent over the angular range  $\theta \leq \arctan(3^{1/2}s)$ , where  $s^2$  is a nominal value of the mean square slope (mss). The limitation of our analysis to  $\theta \leq 10^\circ$  is compatible with this value over the range of winds tested ( $u \geq 5 \text{ m s}^{-1}$ ).

Instead of a diagonal matrix involving both Fresnel reflection coefficients  $R_{HH}^{(0)}$  and  $R_{VV}^{(0)}$ , the coherent re-

flection matrix including the zero- and second-order fields is obtained by Yueh et al. (1994):

$$[R] = \begin{bmatrix} R_{HH} & R_{HV} \\ R_{VH} & R_{VV} \end{bmatrix} = \begin{bmatrix} R_{HH}^{(0)} + R_{HH}^{(2)} & R_{HV}^{(2)} \\ R_{VH}^{(2)} & R_{VV}^{(0)} + R_{VV}^{(2)} \end{bmatrix}, \quad (3)$$

where  $R_{\alpha\beta}^{(2)}$ , with  $\alpha$  and  $\beta$  being V or H, are the second-order corrections of the specular reflection coefficients caused by small surface perturbation. They are given by Yueh (1997) as a function of incidence and azimuth angles  $\theta_i$  and  $\phi_i$  as

$$R_{\alpha\beta}^{(2)}(\theta_i, \phi_i) = \int_0^{2\pi} \int_0^\infty k_o^2 \times F_s(k_{\rho i} \cos \phi_i - k_\rho \cos \phi, k_{\rho i} \sin \phi_i - k_\rho \sin \phi) \cdot g_{\alpha\beta}^{(2)} k_\rho dk_\rho d\phi, \quad (4)$$

where  $k_{\rho i} = k_o \sin \theta_i$  and  $F_s(k, \phi)$  [written as a function of Cartesian coordinates in Eq. (4)] is the small-scale sea wave spectrum, defined as equal to the sea wave spectrum  $F(k, \phi)$  for  $k$  higher than the cutoff wavenumber  $k_d$ , and equal to zero otherwise. The sea wave spectrum  $F(k, \phi)$  is normalized so that  $h^2 = \int_0^{2\pi} \int_0^\infty F(k, \phi) k dk d\phi$ , where  $h^2$  is the mean square height of the waves. The second-order scattering coefficients  $g_{\alpha\beta}^{(2)}$  are functions of permittivity and geometry, and given by Yueh (1997). The complex permittivity is taken from Ellison et al. (1998), assuming a sea surface temperature (SST) of  $10^\circ\text{C}$  and a sea surface salinity (SSS) of 35 practical salinity units (psu). Increasing SST to  $15^\circ\text{C}$ , or SSS to 36 psu, would increase  $|R'(0)|^2$  by 0.02 dB and  $2 \times 10^{-4}$  dB, respectively, which would not lead to significant modifications of the results of this study. In practice, the precise operating frequency of a Ku-band radar, although close to 14 GHz, depends upon the instrument. The nominal runs of the model have been performed here for a frequency  $f_o = 14 \text{ GHz}$ , but in order to explore the sensitivity to the choice of the operating frequency, other tests were performed at slightly different frequencies. The effect of this modification is weak, as will be discussed in section 4.

In this paper, the diffraction-modified reflection coefficient  $R'(0)$  introduced in the two-scale quasi-specular model [Eq. (1)] is identified with the specular reflection coefficient including corrections up to the second order. Thus,  $|R'(0)|^2$  is expressed as

$$|R'(0)|^2 = |R_{\alpha\alpha}^{(0)}(0, \phi) + R_{\alpha\alpha}^{(2)}(0, \phi)|^2. \quad (5)$$

For the anisotropic sea spectrum,  $|R'(0)|^2$  will be slightly dependent on  $\phi$  and on polarization  $\alpha$ . Since only azimuthally averaged values of  $\sigma^o$  are included in

our analysis, we take the mean of  $|R'(0)|^2$  over azimuth  $\phi$ . The result is independent upon whether  $\alpha = H$  or  $V$ .

### 3. Empirical model functions

#### a. Nadir model functions $\sigma^\circ(\theta = 0)$

Providing accurate absolute calibration of  $\sigma^\circ$  is a difficult task. Empirical model functions for  $\sigma^\circ$  at nadir were first developed for the *Seasat* altimeter (Chelton and McCabe 1985; Chelton and Wentz 1986). Chelton and Wentz (1986) also reported a general bias of  $-0.5$  dB of  $\sigma^\circ$  estimates from *Seasat* altimeter (ALT) data as compared to scatterometer (SASS) data at nadir, for situations where  $\sigma^\circ$  is greater than about 10.5 dB. This bias was shown by Chelton et al. (1989) to be due to the use of a flat-earth approximation, which had been used to determine the altimeter footprint area.

A further study involving cross calibration between *Geosat* and *Seasat* altimeter estimates of  $\sigma^\circ$  was performed by Witter and Chelton (1991). They reached the conclusion that the *Seasat* altimeter estimates of  $\sigma^\circ$  were miscalibrated for values of  $\sigma^\circ \leq 11$  dB and proposed a modification to the altimeter model function previously proposed by Chelton and Wentz (1986). This was called by Witter and Chelton the modified Chelton and Wentz (MCW) model function.

Comparing TOPEX/Poseidon and *Geosat* altimeter measurements of  $\sigma^\circ$ , Callahan et al. (1994) identified an offset between both instruments. Callahan et al. mentioned that TOPEX used a round earth correction, which was not used for *Geosat*. If this correction were applied, the *Geosat*  $\sigma^\circ$  would be 0.5 dB higher. Also, unlike *Geosat*, the TOPEX values have an additional correction for atmospheric absorption applied. The minimum absorption correction is about 0.2 dB at Ku band. To minimize the rms difference between the TOPEX and *Geosat* data, Callahan et al. indeed found that an offset of 0.7 dB between both datasets should be introduced. Callahan et al.'s (1994) conclusion is thus that the use of the MCW model function, with a + 0.7 dB offset added in order to account for a round earth and atmospheric corrections, should provide an accurate estimate of  $\sigma^\circ$  at nadir at Ku band as a function of wind speed.

From an analysis performed on the basis of 1 yr of  $\sigma^\circ$  measurements from the TRMM PR radar, Freilich and Vanhoff (2003) obtained a new model function for  $\sigma^\circ(\theta = 0)$ . Following Freilich and Challenor (1994), they expressed their new model function by means of a four-parameter expression. Performing a nonlinear least squares fit of the coefficients to the TRMM PR data, they obtained

$$[\sigma^\circ(\theta = 0)]_{\text{dB}} = 14.08 - 0.2375u + 10.92 \exp(-0.7371u), \quad (6)$$

where  $u$  is the neutral stability wind at 10-m height, expressed in meters per second.

The model function from Freilich and Vanhoff (2003), as well as the MCW model function, are shown in Fig. 1. As was mentioned by Freilich and Vanhoff, it turns out that their model is very similar to the MCW model, except that it exhibits a +1.9 dB offset compared to MCW. Callahan et al.'s (1994) model is also plotted in Fig. 1. As mentioned above, Callahan et al.'s model is identical to the MCW model, except for a +0.7 dB offset to account for a round earth and atmospheric corrections.

It should be mentioned that a two-parameter nadir  $\sigma^\circ$  model function, including the effects of both wind speed and wave height, has been developed by Gourrion et al. (2002) from the TOPEX altimeter observations. Such a refined two-parameter model function, elaborated for the TOPEX altimeter, is unfortunately not available for the other satellites (*Geosat* or TRMM PR). In the present paper, where we are concerned with the comparison between model functions obtained from various satellites, such effects of wave conditions (including either fetch-limited situations or situations with swell) are therefore not studied. We limit ourselves to using the one-parameter model functions  $\sigma^\circ(u)$  built from satellite observations, and we assume that they may be considered to be representative of fully developed situations.

#### b. Shape of the $\sigma^\circ(\theta)$ profile

In the limit of a Gaussian isotropic sea surface slope distribution, the quasi-specular radar cross section from the sea surface is given by Eq. (2) and rewritten here as follows:

$$\sigma^\circ(u, \theta) = \frac{\sigma^\circ(u, \theta = 0)}{\cos^4 \theta} \exp\left[-\frac{\tan^2 \theta}{s^2(u)}\right], \quad (7)$$

where the effective mean square slope  $s^2$  accounts for ocean waves whose wavenumbers are smaller than the scale separation wavenumber  $k_d$ . Jackson et al. (1992) obtained empirical determinations of  $s^2$  by fitting the shape of the profile given by Eq. (7) to the observations. Similarly, Freilich and Vanhoff (2003) were able to infer effective mean square slopes from fits to PR data and gave an accurate parameterization of  $s$  for  $5 \leq u \leq 17$  m s<sup>-1</sup> according to

$$s^2(u) = 0.016 + 0.0016u. \quad (8)$$

Beyond  $u = 17$  m s<sup>-1</sup>, the simple expression (8), how-

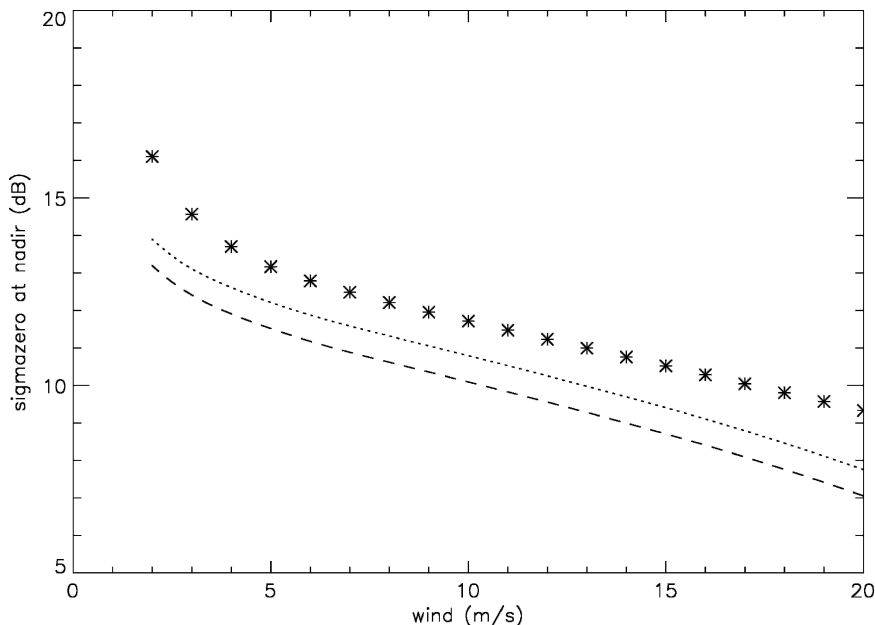


FIG. 1. Empirical model functions for the nadir  $\sigma^\circ$  as a function of wind speed, as given by Freilich and Vanhoff (2003) (stars), Witter and Chelton (1991) (MCW model, dashed line), and Callahan et al. (1994) (dotted line).

ever, becomes less accurate (see Freilich and Vanhoff's Fig. 7), and therefore for the highest wind speed studied here ( $u = 20 \text{ m s}^{-1}$ ),  $s^2(u)$  was taken as 0.046 to be consistent with Freilich and Vanhoff's Fig. 7 [instead of 0.048 as would result from Eq. (8)].

It is to be noted that, in order to determine  $s^2$ , Freilich and Vanhoff's fits were performed using  $\sigma^\circ$  in natural, not decibel, units. Owing to the rapid monotonic decrease of  $\sigma^\circ$  with  $\theta$ , the fit is therefore most sensitive to small incidence angles, where  $\sigma^\circ$  is large. By this way, the authors show that the quality of the fits is excellent for  $\theta \leq 10^\circ$  at all wind speeds, even though the fit was formally performed over a wider range of incidence angles.

In this paper, we use Freilich and Vanhoff's (2003) empirical model function as a reference for radar cross section, obtained by combining Eqs. (6)–(8).

#### 4. Applying the electromagnetic model to the empirical model functions

##### a. Standard method

For every wind speed, we compute the theoretical function  $\sigma^\circ(\theta)$  from the electromagnetic model described in section 2. For this purpose, it is necessary to determine the diffraction-modified Fresnel coefficient  $|R'(0)|^2$ , as well as the slope variance  $s^2$  of the low-pass-filtered surface. The former may be deduced from Eqs.

(4) and (5), provided that the sea wave spectrum  $F(\mathbf{k})$  is known for  $k \geq k_d$ . As for the slope variance  $s^2$ , it may be readily computed by integration of  $k^2 F(\mathbf{k})$  over the range  $k \leq k_d$ . Thus the knowledge of the whole sea wave spectrum  $F(\mathbf{k})$  is required in order to determine  $\sigma^\circ(\theta)$ .

Several spectral models of the sea surface are available in the literature (Donelan and Pierson 1987; Apel 1994; Elfouhaily et al. 1997; Lemaire et al. 1999; Kudryavtsev et al. 1999). In this paper, fully developed situations are assumed, and Elfouhaily et al.'s (1997) model is used. The reason for this choice, as well as trials performed with other spectral models, will be discussed in section 4b below.

To avoid an unphysical negative value of Elfouhaily et al.'s Phillips–Kitaigorodskii equilibrium range parameter for short waves  $\alpha_m$  at low wind, we have followed Freilich and Vanhoff's approach, which consists of replacing Elfouhaily et al.'s two-regime logarithmic law for  $\alpha_m$  with

$$\alpha_m = 0.014u^*/c_m \quad \text{for } u^* \leq 0.308 \text{ m s}^{-1} \quad \text{and} \quad (9a)$$

$$\alpha_m = 0.01[1 + 3 \ln(u^*/c_m)] \quad \text{for } u^* \geq 0.308 \text{ m s}^{-1}, \quad (9b)$$

with  $c_m = 0.23 \text{ m s}^{-1}$  corresponding to the capillary-gravity phase speed minimum.

Also, in order to determine the friction velocity  $u^*$

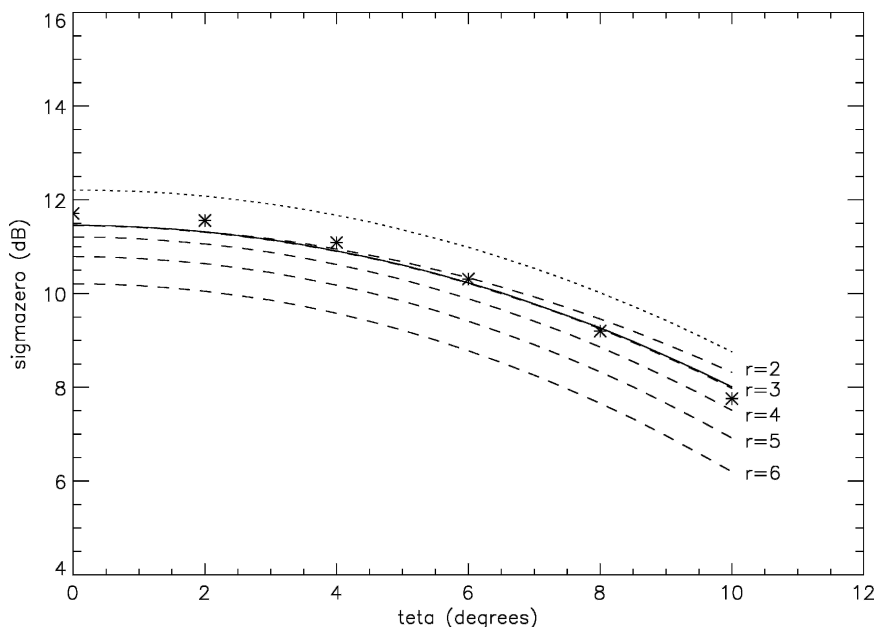


FIG. 2. The  $\sigma^{\circ}$  as a function of incidence angle  $\theta$ , as given by the Freilich and Vanhoff (2003) model function for  $u = 10 \text{ m s}^{-1}$  (stars). Dashed lines show results of the electromagnetic quasi-specular two-scale model, plotted for different values of the assumed ratio  $r = k_o/k_d$ , from  $r = 2$  to 6. The solid line shows the results of the electromagnetic model obtained by taking the value of  $r$  that gives the best fit to the Freilich and Vanhoff model function ( $r = 2.95$ ). The dotted line shows  $\sigma^{\circ}$  obtained with  $r = 2.95$ , but using the nominal (uncorrected) Fresnel coefficient.

for a given  $u$ , the parameterized polynomial form of the 10-m neutral drag coefficient developed by Taylor and Yelland (2001) was used.

Once the sea wave spectrum is determined, the two-scale electromagnetic model can be run, provided that a value of the scale-separation wavenumber  $k_d$  is given. We have chosen to give no a priori information on  $k_d$  and, therefore, we leave it as a free parameter. The value of  $k_d$  is adjusted so as to minimize the rms error  $E$  between the output of the electromagnetic model and the empirical model function of  $\sigma^{\circ}$ .

An example of the fit obtained for  $u = 10 \text{ m s}^{-1}$  is given in Fig. 2. To see how much the modeled  $\sigma^{\circ}$  is sensitive to the choice made for the ratio  $r = k_o/k_d$ , the modeled  $\sigma^{\circ}$  is plotted for different assumptions from  $r = 2$  to  $r = 6$ . Here the best-fitted value of  $r$  is found to be  $r = 2.95$ , and the rms error of the fit is then  $E = 0.19 \text{ dB}$  for  $\sigma^{\circ}$ . As a comparison,  $\sigma^{\circ}$  obtained with  $r = 2.95$ , but using the nominal (uncorrected) Fresnel coefficient, is also plotted as the dotted line in Fig. 2. Note that the correction to the Fresnel coefficient introduced by the second-order term in Eq. (5) reduces  $\sigma^{\circ}$  by 0.75 dB in that case. This effect increases as the ratio  $r = k_o/k_d$  increases. Thus, for the same wind speed  $u = 10 \text{ m s}^{-1}$ , if a ratio  $r = 6$  were taken, the correction to the

Fresnel coefficient due to the second-order term would become as high as 2.6 dB.

For other wind speeds between 5 and  $20 \text{ m s}^{-1}$ , similar fits are obtained, with rms errors ranging from  $E = 0.12$  to  $E = 0.23 \text{ dB}$ . Freilich and Vanhoff mention that TRMM Microwave Imager (TMI) measurements, which they used to estimate wind speeds, underpredict wind speed below  $3 \text{ m s}^{-1}$ , and therefore their inferred effective mean square slope  $s^2(u)$  is probably inaccurate below  $3 \text{ m s}^{-1}$ . Additional effects such as non-Gaussian peakedness (Chapron et al. 2000), which have not been considered here, may also become nonnegligible, and therefore such low wind speeds were not considered here.

Due to the shape of the empirical model function as a function of  $\theta$  [Eq. (7)], which is identical to the theoretical electromagnetic model function,  $E$  should always be exactly equal to 0. The example of Fig. 2 shows, however, that  $E$  is generally not equal to 0, because the fit must also ensure that the computed absolute level of  $\sigma^{\circ}$  coincides with the level of the empirical model function. Thus, for example in Fig. 2, the computed  $\sigma^{\circ}$  (solid line) is slightly too low for small values of  $\theta$  and slightly too high for  $\theta$  approaching  $10^{\circ}$ . Taking the model function by Freilich and Vanhoff (2003) as a reference, we

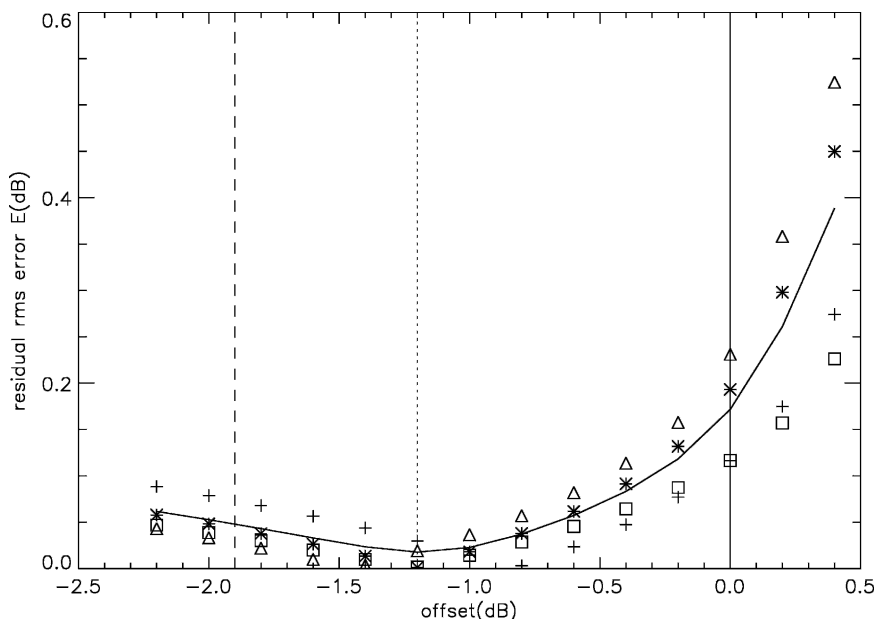


FIG. 3. Residual rms error  $E$  between the best-fitted electromagnetic model and the offset Freilich and Vanhoff model, over the range  $0^\circ \leq \theta \leq 10^\circ$ , plotted as a function of the offset, for  $u = 5$  (plus signs),  $10$  (asterisks),  $15$  (triangles), and  $20 \text{ m s}^{-1}$  (squares). Quadratic mean  $\langle E \rangle$  of the four previous values of  $E$  (solid line). The vertical lines correspond to zero offset (uncorrected Freilich and Vanhoff model function, solid vertical line),  $-1.9 \text{ dB}$  offset (MCW model function, dashed line), and  $-1.2 \text{ dB}$  offset (Callahan et al. model function, dotted line).

have therefore performed the fit of the electromagnetic model to the empirical model function, introducing an offset to the empirical model function, and the residual error  $E$  was computed as a function of the offset. The results are displayed in Fig. 3. For every wind speed, it can be seen that  $E$  tends to decrease when a negative offset is introduced. Depending on the wind speed, a minimum  $E = 0$  is attained for an offset between  $-0.8$  and  $-1.4 \text{ dB}$ , although no clear systematic dependence of this optimum offset with wind speed is noticeable (extreme values of the optimal offset are obtained for  $u = 5$  or  $15 \text{ m s}^{-1}$ , while intermediate values are obtained for  $u = 10$  or  $20 \text{ m s}^{-1}$ ). Denoting as  $\langle E \rangle$  the quadratic mean of  $E$  over the range  $5 \leq u \leq 20 \text{ m s}^{-1}$  (solid line in Fig. 3),  $\langle E \rangle$  is of the order of  $0.17 \text{ dB}$  for zero offset, while the minimum of  $\langle E \rangle$  is attained for an overall offset of  $-1.2 \text{ dB}$ .

As mentioned by Freilich and Vanhoff (2003), their model is virtually  $1.9 \text{ dB}$  above the MCW model, while Callahan et al.'s (1994) model is  $0.7 \text{ dB}$  above MCW (see section 3a). The offsets corresponding to each of the three models discussed here are indicated as straight vertical lines in Fig. 3. It turns out that Callahan et al.'s (1994) model coincides exactly with the minimum of the quadratic mean error  $\langle E \rangle$ , while the MCW model is too low. It may be concluded that, under the standard assumptions made here, there is virtually per-

fect consistency between the absolute calibration proposed by Callahan et al. (1994) and standard electromagnetic modeling.

It should be recalled that the computations were performed here for a radar frequency taken as  $f_o = 14 \text{ GHz}$ . Shifting the frequency to  $f_o = 13.8 \text{ GHz}$  (the one of the TRMM PR) would lead to a slight shift of the optimal offset to  $-1.1 \text{ dB}$  (instead of  $-1.2 \text{ dB}$ ), but would not change qualitatively the results obtained here.

The values obtained for the ratio  $r = k_o/k_d$  between the electromagnetic wavenumber and the scale-separation wavenumber, when an offset of  $-1.1 \text{ dB}$  is introduced, are displayed in Fig. 4. It is of the order of  $7.4$  for  $u = 5 \text{ m s}^{-1}$ , tends to decrease with increasing wind speed, and reaches about  $4.1$  for  $u = 20 \text{ m s}^{-1}$ . Such values are in basic agreement with, although slightly higher than, the values estimated by Jackson et al. (1992), who found  $r$  to be of the order of  $3\text{--}6$  from a Ku-band airborne radar altimeter.

It may be noted that for the SPM method discussed in section 2b to be applicable, the short-scale rms height  $h_s = [\int_0^{2\pi} \int_{k_d}^\infty F_s(k, \theta) k dk d\phi]^{1/2}$  should verify the criterion (e.g., Barrick and Peake 1968)

$$k_o h_s \cos \theta \ll 1. \tag{10}$$

With increasing wind speed, the sea surface roughness



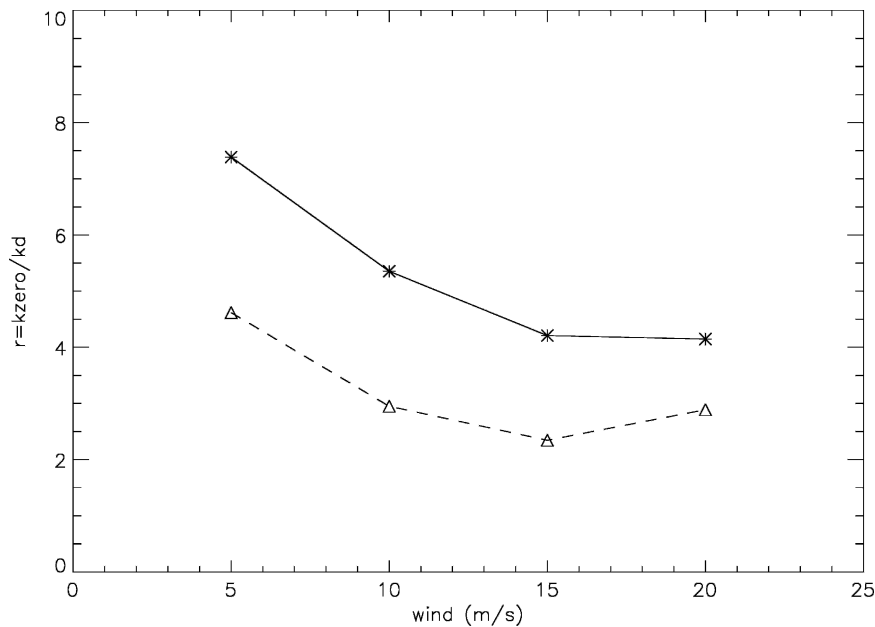


FIG. 4. Ratio  $r = k_o/k_d$  obtained for the best-fitted solution, as a function of wind speed, when an offset of  $-1.1$  dB is assumed (optimal solution for  $f_o = 13.8$  GHz, solid line and asterisks), or when no offset is assumed (uncorrected Freilich and Vanhoff model function, dashed line and triangles).

increases. Since  $h_s$  is obtained by integrating the sea wave spectrum over wavenumbers  $k \geq k_d$ , the separation wavenumber  $k_d$  ought to increase (and therefore  $r = k_o/k_d$  should decrease) to maintain  $h_s$  at a moderate value in such a way that the criterion (10) continues to be verified. The variation of  $r$  with wind speed exhibited in Fig. 4 thus follows the same trend as the variation of the limit of validity of the SPM method with wind speed. We may mention, too, that computations of  $h_s$  performed with the values of  $r$  found here give the inequality (10), which is well verified over the whole range of winds studied.

Finally, as a comparison, the ratio  $r$  for an offset of 0 dB, also indicated in Fig. 4, would be lower by a factor of 1.4–1.6.

#### b. Role of the wave spectral model

As mentioned above, the sea wave spectral model used in this study is Elfouhaily et al.'s (1997) model. It was chosen here both because of its simplicity and for the fact that it is consistent with a variety of high-quality nonradar measurements, including Jähne and Riemer's (1990) laser slope gauge data and Cox and Munk's (1954) measurements of mean square slope (see Elfouhaily et al.'s Fig. 7b), which is an essential parameter as far as radar altimetry is concerned. As a comparison, the mean square slopes of Donelan and Pierson's

(1987) and Apel's (1994) models at  $10 \text{ m s}^{-1}$  are, respectively, 2.4 and 1.4 times the ones of Cox and Munk's clean sea model. Although some artifacts of Elfouhaily's model were identified for L-band radiometric models (Dinnat et al. 2003), Anderson et al. (2002) mentioned that the qualitative agreement of the altimeter cross section obtained with different wave spectra (including Elfouhaily et al.'s model) could not be distinguished at Ku band.

To assess the role of the shape of the wave spectral model used in this study, we performed trials using Apel's (1994) model. However, in order to be consistent with Cox and Munk's (1954) mean square slope measurements, Apel's (1994) model was rescaled by a proportionality factor (depending upon wind speed). Compared to Fig. 3, the results (not shown) then give a much larger rms residual error, with a minimum attained for an offset that is highly dependent upon wind speed. When averaged over wind speed, the residual rms error reaches a minimum of 0.95 dB (to be compared to 0.02 dB obtained with Elfouhaily et al.'s model, as seen in Fig. 3), even though the offset corresponding to this minimum is only slightly modified ( $-1.0$  instead of  $-1.2$  dB). Clearly these results cannot be interpreted in terms of a mere calibration offset. When Donelan et al.'s model, rescaled by the same method, is used, a strong variability of the rms residual error is again obtained and, when averaged over wind

speeds, an unrealistic optimal offset of less than  $-2.2$  dB is found. Thus, the shape of the spectral model plays a significant role, and an accurate knowledge of the spectral shape of the sea surface, indeed constitutes an issue to be addressed in order for this method to become fully reliable. However, the fact that virtually the same optimal offset was found for the various wind speeds tested (from  $5$  to  $20 \text{ m s}^{-1}$ ), as displayed in Fig. 3, and the fact that the optimal residual rms error was extremely low ( $0.02$  dB) give some good confidence for the choice made of Elfouhaily et al.'s model.

*c. Role of peakedness of the sea surface*

Chapron et al. (2000) showed that the peakedness of the sea surface, caused by a fourth-order correction to the sea surface slope pdf  $p(\zeta, 0)$ , affects the absolute level of  $\sigma^\circ$  at nadir, as well as the  $\sigma^\circ(\theta)$  profile. Those authors interpret non-Gaussian peakedness by considering the sea surface as being composed of patches where the sea surface is locally Gaussian, but assuming that the slope variance varies from patch to patch. They show that, because of those fluctuations in  $s^2$ , our Eq. (2) should be replaced by the following more exact quasi-specular expression for  $\sigma^\circ$ :

$$\sigma^\circ(\theta) = \frac{|R'(0)|^2}{s^2 \cos^4 \theta} \exp[-\tan^2 \theta (1 + \Delta)/s^2 + \Delta(1 - \Delta) \tan^4 \theta / s^4 + \dots], \quad (11)$$

where  $\Delta$  is the variance of  $s^2$ . Also, Chapron et al. use the zero-order Fresnel coefficient  $|R^{(0)}(0)|^2$  instead of the diffraction-modified Fresnel coefficient  $|R'(0)|^2$  used in Eq. (11).

Thus two different explanations of the behavior of  $\sigma^\circ$  at low incidence angles are proposed. In the present paper, the effective reflection coefficient is explained by second-order scattering due to subfacet roughness while Chapron et al. explain it by peakedness effects.

On the basis of the analysis of Cox and Munk (1954) and Cox and Munk (1956), Chapron et al. suggest a value of  $\Delta$  independent of wind and estimated as  $\Delta = 0.23$ . The electromagnetic model was thus run, keeping Elfouhaily et al.'s (1997) spectral model but now using Eq. (11) with  $\Delta = 0.23$ . As compared to the overall optimal fit of  $-1.2$  dB obtained in Fig. 3, the result (not shown) then gives an optimal fit for an offset that depends slightly on wind speed (between  $-0.3$  and  $+0.1$  dB), with an average of  $-0.2$  dB. The corresponding ratio  $r$  is between  $4.3$  and  $2.3$  depending upon wind speed. In that case the model function giving the best consistency with the electromagnetic modeling would be that of Freilich and Vanhoff.

It should be noted, however, that the fourth-order coefficients of the Gram–Charlier development of the slope pdf (from which  $\Delta$  can be evaluated) were obtained by Cox and Munk (1954) with a large uncertainty ( $c_{40} = 0.4 \pm 0.2$ ,  $c_{22} = 0.1 \pm 0.05$ ,  $c_{04} = 0.2 \pm 0.4$ ). Cox and Munk also mention that it is possible that systematic errors in the correction for background light may account for much of the observed peakedness. In view of Cox and Munk's inability to measure the steep slopes, Chapron et al. suggest that alternate measurements to clarify variability and magnitude of  $\Delta$  would be beneficial. A complete treatment of the problem including both the diffraction-modified reflection coefficient and peakedness effects would indeed require an accurate evaluation of  $\Delta$  as a function of  $u$ , which is unfortunately not available at this time. The consequence is that we cannot exclude the possibility that, due to peakedness effects, the offset required to match the Freilich et al. model would be smaller (in absolute value) than the  $-1.1$  dB that we found in section 4a in a context where peakedness effects were assumed negligible.

**5. Conclusions**

We have assessed the consistency between empirical Ku-band altimeter model functions of near-nadir normalized radar cross-sectional  $\sigma^\circ$  and electromagnetic two-scale quasi-specular theory in the context of a standard sea wave spectral model. Three kinds of empirical  $\sigma^\circ$  model functions were tested: (i) the modified Chelton and Wentz (MCW) model (Witter and Chelton 1991) based on *Geosat* and *Seasat* altimeter data; (ii) the Callahan et al. (1994) model, which simply consists of adding a  $+0.7$  dB offset to the MCW model, in order to account for a round earth correction as well as atmospheric attenuation, and brings consistency between the *Geosat* and TOPEX absolute calibrations; and (iii) the Freilich and Vanhoff (2003) model, which is based upon the more recent measurements from the TRMM PR instrument. For these three models, the nadir model functions describing the variation of  $\sigma^\circ$  as a function of wind speed are basically very similar, except that they differ by the level of absolute calibration. In short, when compared to TOPEX, *Geosat* is biased by  $-0.7$  dB while TRMM PR is biased by  $+1.2$  dB.

Assuming a sea wave spectrum similar to that used in Elfouhaily et al. (1997), the two-scale quasi-specular electromagnetic model was run, with a wave separation wavenumber  $k_d$  adjusted so as to minimize the rms difference between a theoretical  $\sigma^\circ(\theta)$  function and an empirical near-nadir model function. The quality of the best-fit solution is not perfect, because the shape and

absolute level of the function  $\sigma^{\circ}(\theta)$  cannot usually be adjusted simultaneously by the electromagnetic model. Taking the TRMM PR model function by Freilich and Vanhoff (2003) as a reference, we have therefore performed the fit again, introducing an offset to the empirical model function, and the residual error was computed as a function of the offset. We have found that the overall quality of the fit is the best when a  $-1.1$  dB offset is introduced to the Freilich and Vanhoff model function. To within  $0.1$  dB, this corresponds to the offset that would be required to match the Callahan et al. (1994) model function. We conclude that, under the standard assumptions made here, there is excellent consistency between the absolute calibration proposed for TOPEX by Callahan et al. (1994) and electromagnetic modeling. It should be noted, however, that the shape of the spectral model used in this study plays a significant role, and similar tests performed with other spectral models (Donelan and Pierson 1987; Apel 1994) instead of Elfouhaily et al.'s model, gave results with much poorer residual errors, which were highly wind dependent, and which therefore cannot be interpreted simply in terms of a mere calibration offset. An accurate knowledge of the spectral shape therefore constitutes an issue to be addressed in future work, but the good consistency obtained (optimal offset virtually independent of wind speed, low optimal residual error) gives some confidence in the choice made here of Elfouhaily et al.'s model.

This work was performed in a context where the effect of the peakedness of the sea surface was assumed negligible. In other words, Chapron et al.'s (2000) peakedness parameter  $\Delta$  was assumed to be sufficiently small to be ignored. When parameter  $\Delta$  is assumed to be independent of wind speed and taken as  $\Delta = 0.23$  as suggested by those authors, the optimal offset is then found to be  $-0.2$  dB, thus indicating that at this time the best consistency with electromagnetic modeling is closer to Freilich and Vanhoff's calibration. Unfortunately the value of  $\Delta$  taken here is rather tentative. A more refined assessment would require accurate measurements of parameter  $\Delta$  involving both magnitude and variability with wind speed. Such accurate measurements are unfortunately not available at this time.

#### REFERENCES

- Anderson, C., and Coauthors, 2000: Study of the impact of sea state on nadir looking and side looking microwave backscatter. Final Report to ESA for Contract 12934/98/NL/GD, 43 pp.
- , J. T. Macklin, C. P. Gommenginger, and M. A. Srokosz, 2002: A comparison of the sea-state sensitivity in empirical and theoretical models of altimeter ocean backscatter. *Can. J. Remote Sens.*, **28**, 475–483.
- Apel, J. R., 1994: An improved model of the ocean surface wave vector spectrum and its effects on radar backscatter. *J. Geophys. Res.*, **99**, 16 269–16 291.
- Barrick, D. E., 1968: Rough surface scattering based on the specular point theory. *IEEE Trans. Antennas Propag.*, **16**, 449–454.
- , and W. H. Peake, 1968: A review of scattering from surfaces with different roughness scales. *Radio Sci.*, **3**, 865–868.
- Callahan, P. S., C. S. Morris, and S. V. Hsiao, 1994: Comparison of TOPEX/POSEIDON  $\sigma^{\circ}$  and significant wave height distributions to Geosat. *J. Geophys. Res.*, **99** (C12), 25 015–25 024.
- Chapron, B., V. Kerbaol, D. Vandemark, and T. Elfouhaily, 2000: Importance of peakedness in sea surface slope measurements and applications. *J. Geophys. Res.*, **105** (C7), 17 195–17 202.
- Chelton, D. B., and P. J. McCabe, 1985: A review of satellite altimeter measurement of sea surface wind speed: With a proposed new algorithm. *J. Geophys. Res.*, **90**, 4707–4720.
- , and F. J. Wentz, 1986: Further development of an improved altimeter wind speed algorithm. *J. Geophys. Res.*, **91** (C12), 14 250–14 260.
- , E. J. Walsh, and J. L. MacArthur, 1989: Pulse compression and sea level tracking in satellite altimetry. *J. Atmos. Oceanic Technol.*, **6**, 407–438.
- , J. C. Ries, B. J. Haines, L.-L. Fu, and P. S. Callahan, 2001: Satellite altimetry. *Satellite Altimetry and Earth Sciences*, L.-L. Fu and A. Cazenave, Eds., Academic Press, 1–131.
- Cox, C., and W. H. Munk, 1954: Statistics of the sea surface derived from sun glitter. *J. Mar. Res.*, **13**, 198–227.
- , and W. Munk, 1956: *Slopes of the Sea Surface Deduced From Photographs of Sun Glitter*. Vol. 6, University of California Press.
- Dinnat, E. P., J. Boutin, G. Caudal, and J. Etcheto, 2003: Issues concerning the sea emissivity modeling at L band for retrieving surface salinity. *Radio Sci.*, **38**, 8060, doi:10.1029/2002RS002637.
- Donelan, M. A., and W. J. P. Pierson, 1987: Radar scattering and equilibrium ranges in wind-generated waves with application to scatterometry. *J. Geophys. Res.*, **92**, 4971–5029.
- Elfouhaily, T., B. Chapron, and K. Katsaros, 1997: A unified directional spectrum for long and short wind-driven waves. *J. Geophys. Res.*, **102** (C7), 15 781–15 796.
- Ellison, W., A. Balana, G. Delbos, K. Lamkaouchi, L. Eymard, C. Guillou, and C. Prigent, 1998: New permittivity measurements of sea water. *Radio Sci.*, **33**, 639–648.
- Freilich, M. H., and P. G. Challenor, 1994: A new approach for determining fully empirical altimeter wind speed model functions. *J. Geophys. Res.*, **99**, 25 051–25 062.
- , and B. A. Vanhoff, 2003: The relationship between winds, surface roughness, and radar backscatter at low incidence angles from TRMM precipitation radar measurements. *J. Atmos. Oceanic Technol.*, **20**, 549–562.
- Gourrion, J., D. Vandemark, S. Bailey, B. Chapron, G. P. Gommenginger, P. G. Challenor, and M. A. Srokosz, 2002: A two-parameter wind speed algorithm for Ku-band altimeters. *J. Atmos. Oceanic Technol.*, **19**, 2030–2048.
- Greco, B., A. Martini, N. Pierdicca, and P. Ciotti, 2000: A novel approach for absolute backscatter calibration of spaceborne altimeters. *Proc. IEEE*, **5**, 2191–2193.
- Jackson, F. C., W. T. Walton, and D. E. Hines, 1992: Sea surface mean square slope from Ku-band backscatter data. *J. Geophys. Res.*, **97** (C7), 11 411–11 427.
- Jähne, B., and K. S. Riemer, 1990: Two-dimensional wave number spectra of small-scale water surface waves. *J. Geophys. Res.*, **95**, 11 531–11 546.

- Kudryavtsev, V. N., V. K. Makin, and B. Chapron, 1999: Coupled sea surface–atmosphere model. 2. Spectrum of short wind waves. *J. Geophys. Res.*, **104** (C4), 7625–7639.
- Lemaire, D., P. Sobieski, and A. Guissard, 1999: Full-range sea surface spectrum in nonfully developed state for scattering calculations. *IEEE Trans. Geosci. Remote Sens.*, **37**, 1038–1051.
- Robinson, M. C., 2000: ENVISAT calibration and validation plan. ESA Doc. PO-PL-ESA-GS-1092, 55 pp.
- Taylor, P. K., and M. J. Yelland, 2001: The dependence of sea surface roughness on the height and steepness of the waves. *J. Phys. Oceanogr.*, **31**, 572–590.
- Valenzuela, G. R., 1978: Theories for the interaction of electromagnetic and oceanic waves—A review. *Bound.-Layer Meteor.*, **13**, 61–85.
- Witter, D. L., and D. B. Chelton, 1991: A Geosat altimeter wind speed algorithm and a method for altimeter wind speed algorithm development. *J. Geophys. Res.*, **96** (C5), 8853–8860.
- Yueh, S. H., 1997: Modeling of wind direction signals in polarimetric sea surface brightness temperatures. *IEEE Trans. Geosci. Remote Sens.*, **35**, 1400–1418.
- , R. Kwok, F. K. Li, S. V. Nghiem, and W. J. Wilson, 1994: Polarimetric passive remote sensing of ocean wind vectors. *Radio Sci.*, **29**, 799–814.